

Cold atom Clocks and Applications

S. Bize, P. Laurent, M. Abgrall,
H. Marion, I. Maksimovic, L. Cacciapuoti, J. Grünert
C. Vian, F. Pereira dos Santos, P. Rosenbusch,
P. Lemonde, G. Santarelli, P. Wolf and A. Clairon
BNM-SYRTE, Observatoire de Paris
61 Avenue de l'Observatoire 75014 Paris, France.

A. Luiten, M. Tobar
The University of Western Australia, School of Physics
35 Stirling Highway, Crawley, Western Australia.

C. Salomon
Laboratoire Kastler Brossel, ENS
24 rue Lhomond, 75005 Paris, France

Abstract

This paper describes advances in microwave frequency standards using laser-cooled atoms at BNM-SYRTE. First, recent improvements of the ^{133}Cs and ^{87}Rb atomic fountains are described. Thanks to the routine use of a cryogenic sapphire oscillator as an ultra-stable local frequency reference, a fountain frequency instability of $1.6 \times 10^{-14} \tau^{-1/2}$ where τ is the measurement time in seconds is measured. The second advance is a powerful method to control the frequency shift due to cold collisions. These two advances lead to a frequency stability of 2×10^{-16} at 50 000 s for the first time for primary standards. In addition, these clocks realize the SI second with an accuracy of 7×10^{-16} , one order of magnitude below that of uncooled devices. In a second part, we describe tests of possible variations of fundamental constants using ^{87}Rb and ^{133}Cs fountains. Finally we give an update on the cold atom space clock PHARAO developed in collaboration with CNES. This clock is one of the main instruments of the ACES/ESA mission which is scheduled to fly on board the International Space Station in 2008, enabling a new generation of relativity tests.

1 Introduction: Einstein's legacy in modern clocks

Modern clocks using laser cooled atoms owe a great deal to the famous 1905 "annus mirabilis" of Einstein. Indeed the three theoretical problems that Einstein beautifully solved in 1905 are key ingredients in current atomic clocks, hundred years after Einstein's work.

1. First the quanta of light, photons, are routinely used to cool atoms to microkelvin temperatures and to confine them in electromagnetic traps. Atom manipulation is a direct application of energy and momentum exchanges between light and matter. At one microkelvin, cesium atoms which form the basis for the current definition of the SI unit of time, the second, move at an average speed of 7 mm.s^{-1} , enabling extremely long observation times and thus precision measurements. On Earth, atomic fountains enable unperturbed ballistic flight with duration approaching one second. Furthermore, every experiment in atomic physics routinely uses the Einstein's photoelectric effect in photodiodes to detect, and control light beams. Furthermore, the concept of photon is intimately connected to the famous Planck relationship $E = h\nu$ between energy, Planck's constant and frequency of electromagnetic radiation, which is of paramount importance in atomic clocks.
2. Second Einstein's theory of brownien motion with the famous relationship $k_B T = D/\alpha$ between temperature, diffusion coefficient and friction coefficient not only proved the existence of atoms, but beautifully applies to Doppler and sub-Doppler laser cooling mechanisms at work in every cold atom experiment [1]. In optical molasses atoms are viscously confined by the bath of photons, they experience a three-dimensional random walk in position and storage times in excess of 10 seconds have been observed for this brownien motion.
3. Third Einstein's theory of special (and later general) relativity introduced a new approach relating space and time, and the fundamental concept of relativistic invariance and Lorentz transformation. Einstein predicted that time in a fast moving frame seems to slow down to someone not moving with it, and distances appear shorter. This revolutionary approach had major fundamental as well as practical consequences in the following century. Clocks in different reference frames tick at different rates and the well-known GPS receivers which equip boats, cars, and planes use routinely Einstein's relativity to determine their position with 10 meter accuracy. Indeed, the atomic clocks onboard the 24

GPS satellites orbiting the Earth at an altitude of 20 000 kms must be corrected for relativistic effects (time dilation and gravitational shift) in order to be synchronized with ground clocks and to reach this positioning accuracy. The correction is about 38 microseconds per day. If each satellite would not apply this compensation the positioning error would reach 11 kilometers per day !

These three papers have had revolutionary consequences in Science and society.

Historically, clocks have played a major role in tests of predictions of relativity theories, from the Hafele-Keating clock transport in jet planes, the Pound-Rebka gravitational shift measurement, the Vessot-Levine GP-A Space hydrogen maser red-shift measurement, and radar ranging Shapiro delay experiment [2]. In addition the current definition of time in the SI unit system, the second, relies on Einstein Equivalence Principle (EEP). This principle is the foundation for all gravitational metric theories that describe gravity as a consequence of curved space-time. The Einstein Equivalence Principle states [2]:

1. if an uncharged test body is placed at an initial event in spacetime and given an initial velocity there, then its subsequent trajectory will be independent of its internal structure and composition
2. In any freely falling frame, the outcome of any local non gravitational test experiments is independent of the velocity of the frame
3. the outcome of any local non gravitational test experiment is independent of where and when in the universe it is performed

An immediate consequence of EEP is that the fundamental constants of physics such as the gravitational constant G , or the fine structure constant $\alpha = e^2/4\pi\epsilon_0\hbar c$ must be independent of time and space.

In this article we first describe recent progress in the realization of the SI second using laser cooled cesium and rubidium clocks. In a second part we use these highly stable devices to perform new tests of Einstein Equivalence Principle, namely the constancy of fundamental constants.

2 Atomic Fountains

The ever increasing control of the motion of atomic samples is at the origin of recent progress in atomic frequency standards and precision measurements

[3]. Laser cooled and trapped atoms enable long observation times required for high precision measurements. Charged particles confined in Paul or Penning traps offer extremely long storage enabling high precision mass measurements, fundamental tests, and the realization of ultra-stable microwave and optical clocks. The recent NPL frequency measurement of an optical transition in Sr^+ ion with an uncertainty of 3×10^{-15} [4] is only a factor three or four worse than the current accuracy of cesium fountains. Precision measurements with neutral atoms on the other hand are usually performed in an atomic fountain where laser cooled atoms ballistically propagate for durations up to one second. In the last decade, atomic clocks and inertial sensors using matter wave interferometry in fountains have become two of the most important applications of cold atoms [3, 5]. About two dozens of fountain devices are now used for a variety of applications. It has been shown recently that microwave and optical clocks as well as matter-wave inertial sensors belong to the same general class of atom interferometers [6]. As an example the current sensitivity in acceleration measurement with atom interferometers is on the order of $3 \times 10^{-8} \text{ m.s}^{-2}$ in one minute measurement duration and, in a decade, cesium fountain clocks have gained almost two orders of magnitude in accuracy. As we show in this paper the fractional inaccuracy of the BNM-SYRTE fountains at Paris Observatory do not exceed today 7×10^{-16} which corresponds to less than a single second error over 50 million years, allowing for the realization of SI unit of time, the second, at the same level. About half a dozen fountains throughout the world at metrology institutes including PTB, NIST, IEN, NPL, have now an accuracy near 10^{-15} , making fountains a major contributor to the accuracy of the TAI (Temps Atomique International). In the future, many applications, such as positioning systems (GPS, GALILEO, GLONASS) as well as scientific applications will benefit from these developments. For instance, deep space satellites have travel durations of several years across the solar system. Precise monitoring of their position requires timescales with very low long term drift. Also, using advanced time and frequency transfer systems (operating at higher carrier frequency and chip rate and/or using two way transfer techniques) may lead to positioning accuracy at the millimeter level for averaging time of a few hundred seconds. This would impact many geodetic applications.

In this paper we show that prospects for further improvements are important. A frequency comparison between two fountains exhibits a stability of 2×10^{-16} at 50 000 second averaging time, for the first time for atomic standards. This frequency resolution sets the stage for clock accuracy at the 10^{-16} level for cesium, almost one order of magnitude potential gain, and even better for rubidium with its far reduced collision shift [7, 8]. We begin by recalling the basic operation of fountain atomic clocks and introduce

several new techniques which demonstrate frequency measurements with a frequency resolution at the 10^{-16} level. The first technique makes use of an ultra-stable cryogenic oscillator to interrogate the clock transition in the fountain. Thanks to its extremely good short term frequency stability and low phase noise, the frequency stability of cesium and rubidium fountains is one order of magnitude below that of fountains using an ultra-stable quartz oscillator as interrogation oscillator. It currently reaches $1.6 \times 10^{-14} \tau^{-1/2}$ where τ is the averaging time in seconds. The fundamental quantum noise of the clock is now reached with atomic samples of up to 10^7 atoms. The second advance deals with a new technique to measure and cancel with high precision the collisional shift in the clock. This shift is a major plague in cesium clocks and is much reduced (two orders of magnitude) in rubidium devices [7, 8]. The method uses interrupted adiabatic population transfer to prepare precise ratios of atomic densities. We show here that the cesium collisional shift can be measured and cancelled at the 10^{-3} level. By comparing rubidium and cesium fountains over a duration of six years, a new upper limit for the drift of fundamental constants has been obtained. Finally we present the development status of the PHARAO cold atom space clock which is under industrial realization. PHARAO will fly onboard the international Space station in the frame of the European ACES mission in 2008-2009 and perform fundamental physics tests such as an improved measurement of Einstein's red-shift, search for drift of fundamental constants and special relativity tests.

3 Recent advances in cesium and rubidium fountains

In this section we briefly review recent advances on cesium and rubidium fountains performed in our laboratory, BNM-SYRTE where three laser cooled atomic fountains are in operation. The first one (FO1), in operation since 1994 [5], has been refurbished recently. The second one (FOM), a transportable fountain, is derived from the PHARAO space clock prototype [9]. This fountain was transported on two occasions to the Max Planck Institute in Garching for direct frequency measurement of the hydrogen $1s \rightarrow 2s$ transition [47](See section on stability of fundamental constants). The third one (FO2), a dual fountain operating with ^{133}Cs or ^{87}Rb , is described in [7]. Here we only briefly describe the present design and recent improvements of FO1 and FO2. A scheme of the fountain apparatus is shown in Fig.1. An optical bench provides through optical fibers all beams required for manipu-

lating and detecting the atoms. The fountains operate with $\text{lin} \perp \text{lin}$ optical molasses. Atoms are cooled by six laser beams supplied by preadjusted fiber couplers precisely fixed to the vacuum tank and aligned along the axes of a 3 dimensional coordinate system, where the (111) direction is vertical. In FOM, optical molasses is loaded from a ^{133}Cs vapor and 3×10^7 atoms are cooled in 400 ms. In FO1 and FO2, optical molasses are loaded from a laser slowed atomic beam which is created by diffusing ^{133}Cs or ^{87}Rb vapor through a bundle of capillary tubes. With this setup 3×10^8 ^{133}Cs atoms can be loaded in 400 ms in FO1. In FO2 an additional transverse cooling of the atomic beam increases the loading rate to 10^9 atoms in 100 ms for ^{133}Cs .

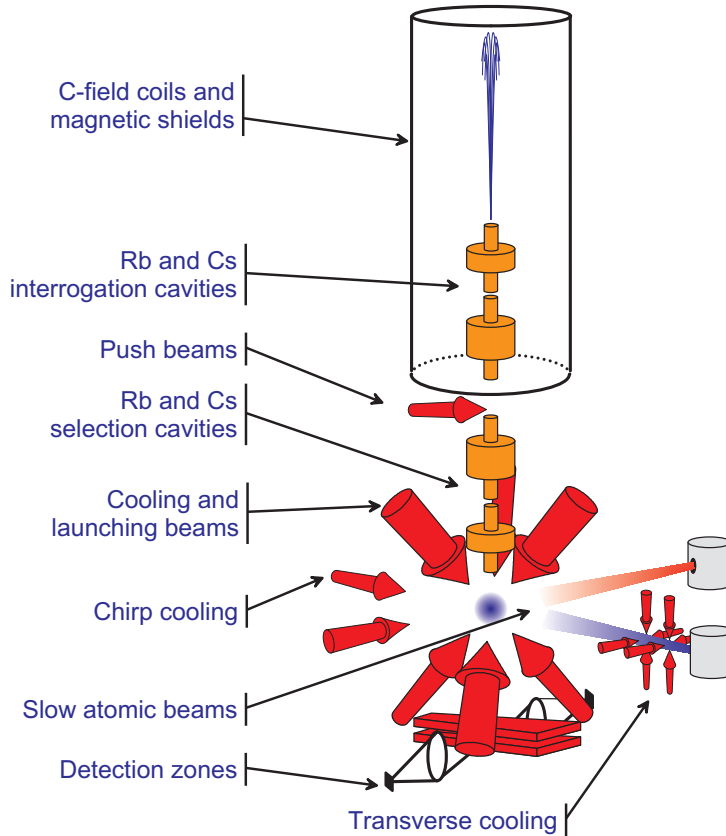


Figure 1: Schematic view of the dual Cs-Rb atomic fountain.

The atoms are launched upwards at $4 \text{ m}\cdot\text{s}^{-1}$ by using moving optical molasses and cooled to $\sim 1 \mu\text{K}$ in the moving frame by adiabatically decreasing the laser intensity and increasing the laser detuning. In normal operation atoms in the clock level $|F = 3, m_F = 0\rangle$ are selected by microwave and light pulses.

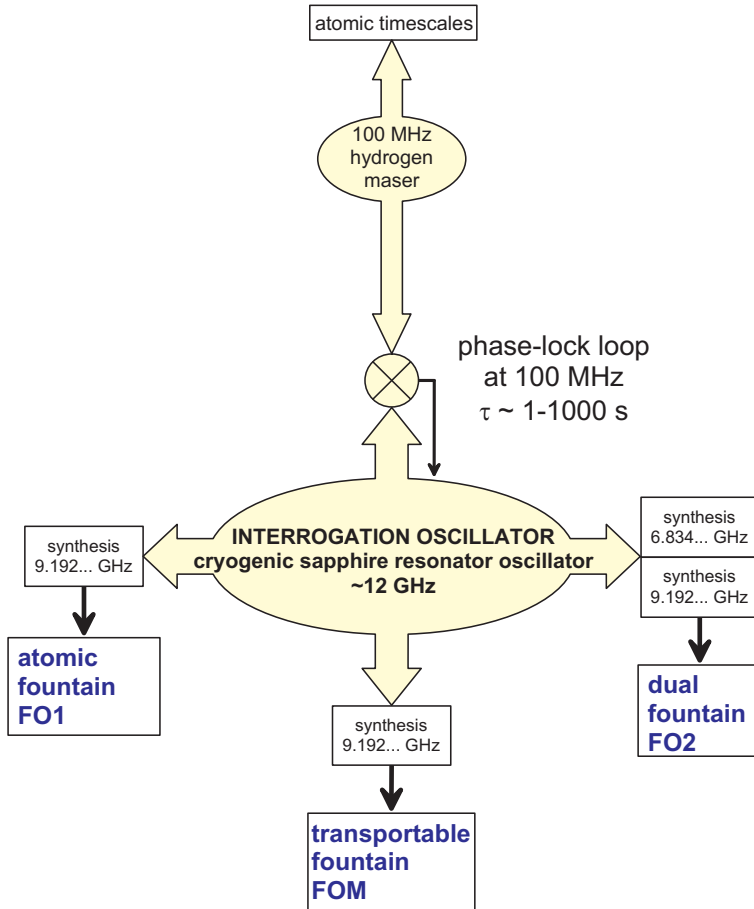


Figure 2: BNM-SYRTE fountain ensemble.

About 50 cm above the capture zone, a cylindrical copper cavity (TE_{011} mode) is used to probe the hyperfine transition in a Ramsey interrogation scheme. The cavities have a loaded quality factor of $Q_{FO1} = 10000$ for FO1 and $Q_{FO2} = 6600$ for FO2. Both cavities can be fed with two coupling irises oppositely located on the cavity diameter. Symmetric or asymmetric feedings are used to evaluate and reduce the residual Doppler effect due to imperfections of the standing wave in the cavity and a tilt of the launch direction of the atoms.

The microwaves feeding the cavities are synthesized from the signal of an ultra-stable cryogenic sapphire resonator oscillator (CSO) developed at the University of Western Australia [10]. As shown in Fig.2, the three fountains use the same CSO oscillator to synthesize the microwave signals probing the atomic transition. To reduce its drift, the CSO is weakly phase-locked

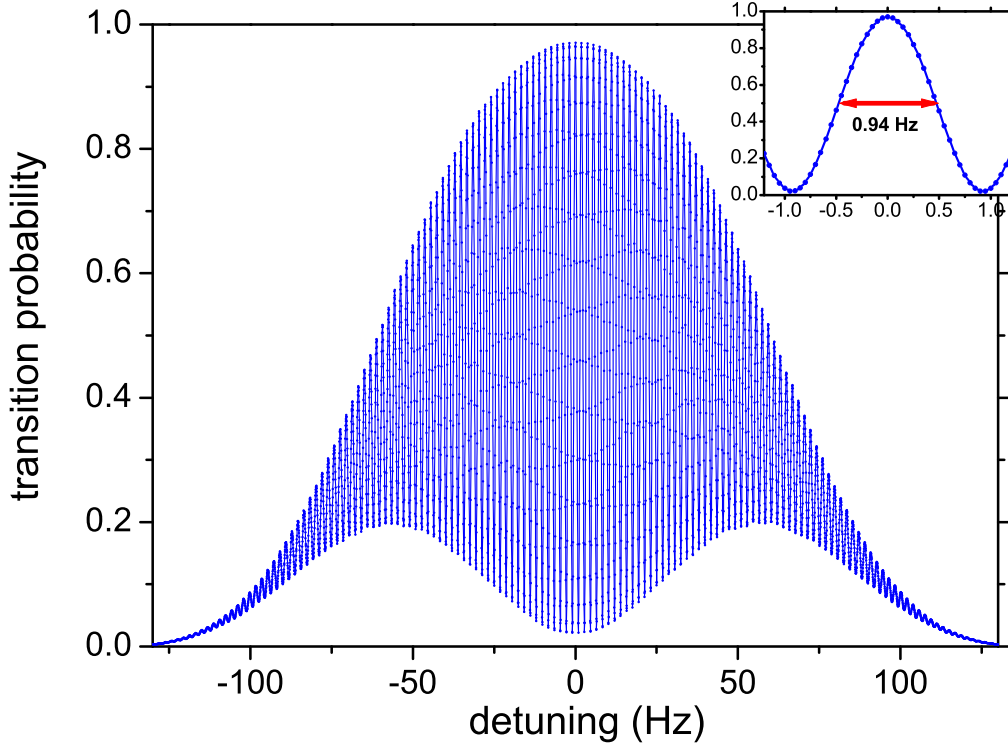


Figure 3: Experimental Ramsey fringes (transition probability as a function of the microwave detuning) measured with ^{133}Cs in FO2 fountain. The insert shows the central fringe with a FWHM of ~ 1 Hz. Each point is a single 1.3 s measurement. At half maximum of the central fringe, the signal to noise ratio is 5 000, within 20% of the fundamental quantum noise with $\sim 10^7$ detected atoms.

to a hydrogen maser. This maser contributes to the local timescale and TAI (Temps Atomique International) through various time and frequency transfer systems. With this setup, atomic fountains are used as primary frequency standard to calibrate TAI and can be compared to other remote clocks. Nowadays, atomic fountains are the dominant contributors to the accuracy of TAI.

The 11.932 GHz output signal from the CSO is converted in order to synthesize 11.98 GHz and 100 MHz signals, both phase coherent with the H-maser. FO2 uses the 11.98 GHz signal to generate 9.192 GHz by a home-build low noise synthesizer which achieves a frequency stability of 3×10^{-15} at 1 s by operating only in the microwave domain. This scheme reduces at the minimum the phase noise and the spurious side-bands induced by the

down conversion process. A similar setup is used to synthesize the 6.834 GHz required for the FO2 fountain operation with ^{87}Rb . The 150 m distance between FO1, FOM and the CSO prevents the direct use of the 11.98 GHz signal. Instead, a 100 MHz signal is synthesized from the CSO and distributed to FO1 and FOM via a high stability RF cable. Finally, a 100 MHz to 9.192 GHz home-made synthesizer generates the interrogation signal. These additional steps degrade the phase noise of the interrogation signal in FO1 and FOM with a frequency stability currently limited to $\sim 2 \times 10^{-14}$ at 1 s.

Frequency stability

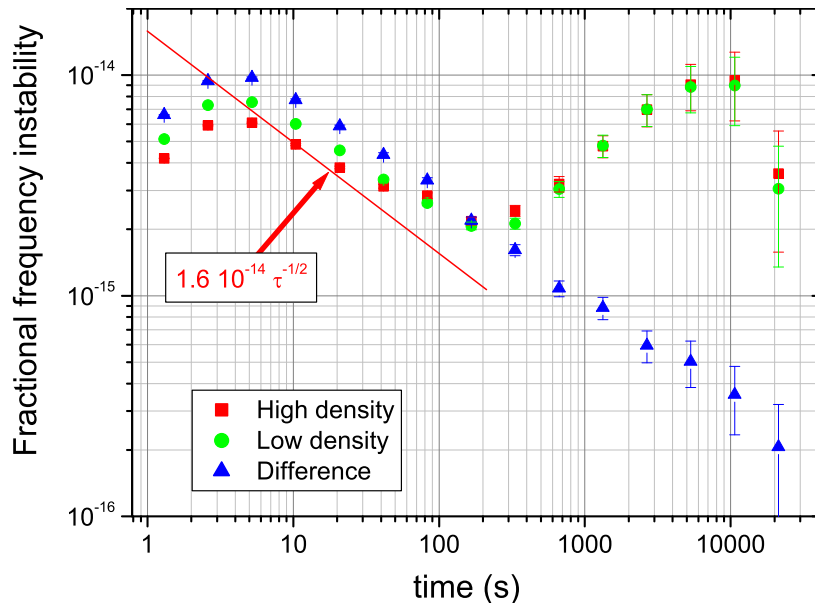


Figure 4: Fractional frequency instability of FO2 against CSO for high density (HD, red squares) and low density (LD, green circles) configurations. It demonstrates a stability of $1.6 \times 10^{-14} \tau^{-1/2}$ for a ^{133}Cs primary standard. Also shown is the fractional frequency instability for the differential measurement between HD and LD (blue triangles). This curve demonstrates an excellent rejection of the CSO fluctuations in the differential measurement, allowing for a fractional frequency resolution of 2.5×10^{-16} at 20 000 s. In this measurement, the collisional shift at LD is the frequency difference between HD and LD ($\sim 5 \times 10^{-14}$). It is obtained with a resolution close to 2 parts in 10^{-16} and it is stable at the 0.5% level over 20 000 s.

Atoms selected in $|F = 3, m_F = 0\rangle$ cross the microwave cavity on the way

up and on the way down, completing the two Ramsey interactions. After the Ramsey interrogation, the populations N_e and N_g of both clock levels $|e\rangle$ and $|g\rangle$ are measured by fluorescence. The number of detected atoms is typically 0.5% of the initially captured atoms. The signal $p = N_e/(N_e + N_g)$ is equal to the atomic transition probability and is insensitive to atom number fluctuations. A typical Ramsey resonance is presented in Fig.3. From the transition probability, measured on both sides of the central Ramsey fringe, we compute an error signal to lock the microwave interrogation frequency to the atomic transition using a digital servo loop. At the quantum limit one expects $S/N = 1/\sigma_{\delta p} = 2\sqrt{N}$ for N detected atoms, where $\sigma_{\delta p}$ is the shot to shot standard deviation of the fluctuations of the transition probability. The frequency corrections are applied to a computer controlled high resolution DDS synthesizer in the microwave generator. These corrections are used for the accuracy and frequency stability evaluations of each fountain. The fractional frequency instability of the FO2 fountain operating with $\sim 10^7$ detected atoms and measured against the cryogenic oscillator is plotted Fig.6. At the quantum limit one expects a frequency instability, characterized by the fractional Allan standard deviation, given by: $\sigma_y(\tau) = (1/\pi Q_{at})\sqrt{T_c/N\tau}$, where $Q_{at} \sim 10^{10}$ is the atomic quality factor, τ and T_c are respectively the averaging time and the cycle duration. Above the servo-loop time constant (~ 3 s) and below 100 s, the fractional instabilities of FO1 and FO2 are $\sigma_y(\tau) = 2.9 \times 10^{-14}\tau^{-1/2}$ and $1.6 \times 10^{-14}\tau^{-1/2}$ respectively, within $\sim 20\%$ of the standard quantum limit. For longer averaging time the frequency instability is dominated by the frequency fluctuations of the CSO and the H-maser. This is the first demonstration of routinely operated primary frequency standards with frequency instabilities in the low $10^{-14}\tau^{-1/2}$ region. We will show below that this excellent short term stability enables an evaluation of systematic frequency shifts and frequency comparisons between clocks at the 10^{-16} level in a few days.

Accuracy

All known systematic frequency shifts are evaluated in our fountains. The accuracy budget for each shift is given in table I for ^{133}Cs . The overall uncertainty, the quadratic sum of all uncertainties is 7.5×10^{-16} for FO1, 6.5×10^{-16} for FO2 and 8×10^{-16} for FOM. In the following, we only discuss some of the most bothersome effects and the recent improvements in their evaluation. A more complete discussion of systematic effects can be found in [11].

Table 1: Systematic fractional frequency shifts for FO1 and FO2.

	FO1 ($\times 10^{16}$)	FO2 ($\times 10^{16}$)	FOM ($\times 10^{16}$)
Quadratic Zeeman effect	1199.7 ± 4.5	1927.3 ± 0.3	351.9 ± 2.4
Blackbody radiation	-162.8 ± 2.5	-168.2 ± 2.5	-191.0 ± 2.5
Collisions and cavity pulling (HD)	-197.9 ± 2.4	-357.5 ± 2.0	-34.0 ± 5.8
Spectral purity & leakage	0.0 ± 3.3	0.0 ± 4.3	0.0 ± 2.4
First order Doppler effect	< 3	< 3	< 2
Ramsey & Rabi pulling	< 1	< 1	< 1
Microwave recoil	< 1.4	< 1.4	< 1.4
Second order Doppler effect	< 0.08	< 0.08	< 0.08
Background collisions	< 1	< 1	< 1
Total uncertainty	± 7.5	± 6.5	± 7.7

Cold collisions and cavity pulling

The cold collision frequency shift is known to be particularly large for ^{133}Cs [12, 13]. For instance, when FO2 is operated at its best frequency stability the shift is $\sim 10^{-13}$. The linear extrapolation of this effect to zero density is known to be delicate. As pointed out in the first paper observing the cold collision shift in ^{133}Cs fountains [12], selecting atoms in the clock levels using microwaves may lead to distortions of the position or velocity distribution. Methods to cope with these effects have been proposed [8], yet the linear extrapolations have proved to be valid only at the 5% to 10% level.

To evaluate the collision shift at the 10^{-3} level (a requirement for a frequency stability and accuracy at 10^{-16}), we recently developed a new method based on interrupted adiabatic passage to select atoms in the $|F = 3, m_F = 0\rangle$ state [14]. Atomic samples are prepared by transferring atoms from $|F = 4, m_F = 0\rangle$ to $|F = 3, m_F = 0\rangle$ with an efficiency precisely equal to 100% (high density, HD) or 50% (low density, LD). With this method, the atom number is changed without affecting either the velocity or the position distributions. Therefore, the density ratio LD/HD is equal to the atom number ratio and is 1/2 at the 10^{-3} level. Since the collisional shift is proportional to the atomic density, it can be extrapolated to zero density with this accuracy. In addition, with this method, the cavity frequency pulling [7, 8, 15] is also accounted for.

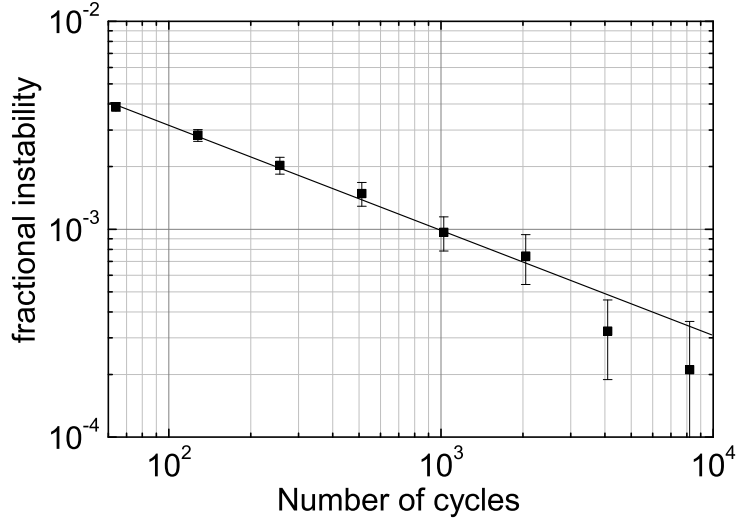


Figure 5: Fractional instability of the ratio of the detected atom number in $|F = 4, m_F = 0\rangle$ between low density and high density configurations as a function of the number of fountain cycles. The measured ratio is $0.5005(2)$. Each cycle lasts ~ 1.3 s. The stability (solid line) decreases as the square root of the number of cycles.

The collisional shift is measured in real-time with the following differential method. The clock is operated alternately in the HD configuration for 60 s and in the LD configuration for the next 60 s. This timing choice minimizes the noise due to frequency instabilities of the CSO oscillator. As seen in Fig.4, at 120 s the stability of FO2 against CSO is near its minimum. Also, over this 120 s period, density fluctuations do not exceed $\sim 1\%$. On the other hand, due to slow changes in the clock environment, we observe that the density may fluctuate up to 10 – 20% over one or several days. Our differential method efficiently cancels these slow daily density variations.

In [14], our calculations predicted that the interrupted adiabatic passage method does provide a LD/HD ratio precisely equal to $1/2$ to better than 10^{-3} . Initially, we were experimentally able to realize this ratio at the 1% level. Improvements in the accuracy of the microwave frequency synthesis for the adiabatic passage enable us to now reach a precision of 2×10^{-3} for this ratio.

During routine operation of the fountains, the number of detected atoms in each hyperfine state is recorded for both LD and HD configurations. As seen in Fig.5, the Allan standard deviation of the measured LD/HD atom number ratio decreases as the square root of the number of fountain cycles

(or time), down to a few parts in 10^4 for one day of averaging. Despite the 10–20% slow drift in atom number over days, this ratio remains remarkably constant. The LD/HD atom number ratio in $|F = 4, m_F = 0\rangle$ is found equal to 1/2 to better than 10^{-3} . This method relies on fluorescence measurements made in the detection zones for each fountain cycle. Various measurements have been performed to establish that the measurement of this ratio is not biased by more than 10^{-3} due optical thickness effects in the detection. On the other hand, the LD/HD atom number ratio in $|F = 3, m_F = 0\rangle$ is found to slightly differ from 1/2 by 0.3% typically. This deviation originates from atoms in the $|F = 3, m_F \neq 0\rangle$ states populated by imperfections in the state preparation. This deviation must be taken into account in the evaluation of the collisional shift. In [16], we showed that the frequency shift of the clock transition due to $|F = 3, m_F \neq 0\rangle$ atoms is at most 1/3 of that of collisions between $|F = 3, m_F = 0\rangle$ and $|F = 4, m_F = 0\rangle$ clock states. Their contribution to the collisional frequency shift is thus at the 0.1% level. In summary, when this adiabatic passage method is used, we take a 2×10^{-3} relative uncertainty for the determination of the high density cold collision shift.

Effect of microwave spectral purity and leakage

Spectral impurities of the interrogation signal and microwave leakage may cause shifts of the clock frequency. In order to evaluate these effects, we make use of their dependance with the microwave power. We alternate the Ramsey interrogation between a configuration of $\pi/2$ and $3\pi/2$ pulses, i.e. a variation of a factor of 9 in microwave power. Within the resolution of the measurement of 3.3×10^{-16} , no frequency shift is observed. In this measurement, four data sets are recorded, LD and HD at $\pi/2$ and LD and HD at $3\pi/2$. In this way, the collisional shift (which may also change with the microwave power) is evaluated and cancelled for both $\pi/2$ and $3\pi/2$ configurations by the differential method described above, allowing for the extraction of a possible influence of microwave spectral purity and leakage alone.

Residual first order Doppler effect

A frequency shift due to the first order Doppler effect can occur if the microwave field inside the interrogation cavity exhibits a phase gradient and the atoms pass the cavity with a slight inclination from the cavity axis. We determine the frequency shift due to the linear component of the phase gradient in a differential measurement by coupling the microwave interrogation

signal “from the left”, “from the right” or symmetrically into the cavity, providing 3 data sets. The observed shift between the “left” and symmetric configuration is $(-25.3 \pm 1.1) \times 10^{-16}$ while the shift between the “right” and symmetric configuration is $(+24.0 \pm 1.2) \times 10^{-16}$. The magnitude of this residual first order Doppler effect is consistent with a simple estimate of the residual traveling wave component in the cavity [17] together with a misalignment between the local gravity and the launch direction $\lesssim 1$ mrad. The mean of these two measurements is $(-0.7 \pm 0.8) \times 10^{-16}$ and consistent with zero, indicating that the traveling wave component is well cancelled in the symmetric coupling configuration. Using the atoms as a probe, we can indeed ensure that the cavity is fed symmetrically to better than 1% in amplitude and 60 mrad in phase, which cancels the effect of linear phase gradient to $\sim 1\%$, better than the above measurement resolution. As a consequence, only the quadratic phase dependence of the microwave field remains as a possible source of residual Doppler shift. A worst case estimate based on [17] gives an upper bound for the fractional frequency shift of 3 parts in 10^{16} , which we conservatively take as the overall uncertainty associated with residual first order Doppler effect.

Other contributions to the accuracy budget are listed in Table 1. The total accuracy currently reaches 7.5 parts in 10^{16} for FO1, 6.5 parts in 10^{16} for FO2, and 8.0 parts in 10^{16} for FOM. This represents a one order of magnitude improvement over uncooled cesium devices. In the future, we anticipate that the extensive use of the methods described above will enable us to bring the accuracy of ^{133}Cs fountains below 2 parts in 10^{16} and the accuracy of ^{87}Rb to a even lower value thanks to its 100-fold lower collision shift [7, 8].

Frequency comparisons between two ^{133}Cs fountains at $2 \cdot 10^{-16}$

The routine operation of two atomic fountains near the quantum noise limit using the CSO as an interrogation oscillator enables frequency comparisons in the low 10^{-16} range, for the first time for primary frequency standards. Figure 6 presents the frequency stability between FO1, FO2 and CSO. Each fountain is operated in differential mode in order to permanently evaluate and cancel the collision shift. Appropriate post-processing of the data thus enables us to construct for each fountain, a clock which is free of the cold collision shift and whose stability is shown in Fig. 6 against the CSO oscillator. Fig. 6 also shows that the combined stability between these two clocks reaches 2.2×10^{-16} at 50 000 s, a previously unattained long term stability. From this data, we infer that at least one of the two fountains has a stability below $(2.2/\sqrt{2}) \times 10^{-16} = 1.6 \times 10^{-16}$ at the same averaging time. The mean

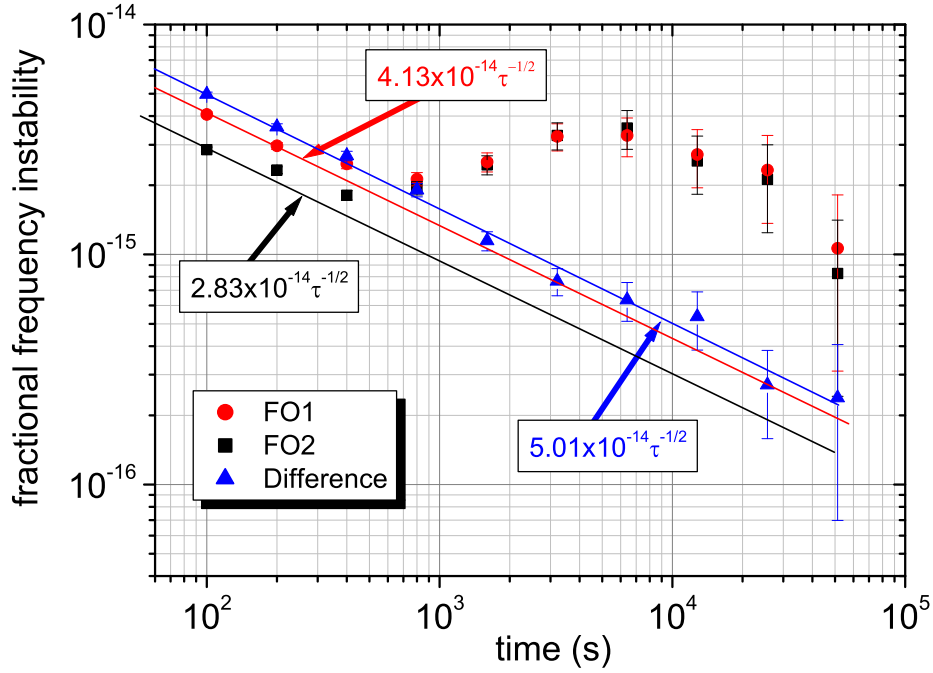


Figure 6: Fractional frequency instability (Allan deviation) between FO1 and FO2 fountains (blue triangles). After 50 000 s of averaging, the stability between the two fountains is 2.2 parts in 10^{16} . Also plotted is the fractional frequency instability of FO1 (red circles) and FO2 (black squares) against the CSO locked to the hydrogen maser.

fractional frequency difference between the two fountains is 4×10^{-16} , fully compatible with the accuracy of each of the two clocks as stated in Table 1. This very good stability sets a new challenge for time and frequency transfer systems between remote clocks. As an example, long distance frequency comparisons between PTB and NIST fountains were performed at the level of only 6×10^{-16} after 2 weeks of averaging with GPS [18]. Similarly, comparisons between BNM-SYRTE and PTB recently achieved 2×10^{-15} for one day of integration with TWSTFT [19].

4 Einstein Equivalence Principle and Stability of fundamental constants

Highly accurate atomic clocks offer the possibility to perform laboratory tests of possible variations of fundamental constants. Such tests interestingly

complement experimental tests of the Local Lorentz Invariance and of the Universality of free-fall to experimentally establish the validity of Einstein's Equivalence Principle (EEP). They also complement tests of the variability of fundamental constants on different timescales, geological timescale [20, 21] and cosmological timescale [22, 23]. Nearly all unification theories (in particular string theories) violate EEP at some level [24, 25, 26] which strongly motivates experimental searches for such violations.

Tests described here are based on highly accurate comparisons of atomic energies. In principle, it is possible to express any atomic energy as a function of the elementary particle properties and the coupling constants of fundamental interactions using Quantum Electro-Dynamics (QED) and Quantum Chromo-Dynamics (QCD). As a consequence, it is possible to deduce a constraint to the variation of fundamental constants from a measurement of the stability of the ratio between various atomic frequencies.

Different types of atomic transitions are linked to different fundamental constants. The hyperfine frequency in a given electronic state of alkali-like atoms (involved for instance in ^{133}Cs , ^{87}Rb [27], $^{199}\text{Hg}^+$ [28, 29], $^{171}\text{Yb}^+$ microwave clocks) can be approximated by:

$$\nu_{\text{hfs}}^{(i)} \simeq R_{\infty} c \times \mathcal{A}_{\text{hfs}}^{(i)} \times g^{(i)} \left(\frac{m_e}{m_p} \right) \alpha^2 F_{\text{hfs}}^{(i)}(\alpha), \quad (1)$$

where the superscript (i) indicates that the quantity depends on each particular atom. R_{∞} is the Rydberg constant, c the speed of light, $g^{(i)}$ the nuclear g-factor, m_e/m_p the electron to proton mass ratio and α the fine structure constant. In this equation, the dimension is given by $R_{\infty}c$, the atomic unit of frequency. $\mathcal{A}_{\text{hfs}}^{(i)}$ is a numerical factor which depends on each particular atom. $F_{\text{hfs}}^{(i)}(\alpha)$ is a relativistic correction factor to the motion of the valence electron in the vicinity of the nucleus. This factor strongly depends on the atomic number Z and has a major contribution for heavy nuclei. Similarly, the frequency of an electronic transition (involved in H [30], ^{40}Ca [31], $^{199}\text{Hg}^+$ [32], $^{171}\text{Yb}^+$ [33, 34] optical clocks) can be approximated by

$$\nu_{\text{elec}}^{(i)} \simeq R_{\infty} c \times \mathcal{A}_{\text{elec}}^{(i)} \times F_{\text{elec}}^{(i)}(\alpha). \quad (2)$$

Again, the dimension is given by $R_{\infty}c$. $\mathcal{A}_{\text{elec}}^{(i)}$ is a numerical factor. $F_{\text{elec}}^{(i)}(\alpha)$ is a function of α which accounts for relativistic effects, spin-orbit couplings and many-body effects ¹.

¹It should be noted that in general the energy of an electronic transition has in fact a contribution from the hyperfine interaction. However, this contribution is a small fraction of the total transition energy and thus carries no significant sensitivity to a variation of

According to [35, 36], the sensitivity to g-factors $g^{(i)}$ and to the proton mass m_p can be related to a sensitivity to fundamental parameters, namely the mass scale of QCD Λ_{QCD} and the quark masses $m_q = (m_u + m_d)/2$ and m_s . Therefore, any measurement of the ratio between atomic frequencies can be interpreted as testing the stability of 4 dimensionless fundamental constants: α , m_q/Λ_{QCD} , m_s/Λ_{QCD} and m_e/Λ_{QCD} . The sensitivity to m_s/Λ_{QCD} is relatively weak compared to the 3 other constants. The sensitivity coefficients have now been calculated for a large number of atomic species used in atomic clocks [28, 35, 37, 38, 39, 40, 41, 36, 42]. Reliable knowledge of these sensitivity coefficient at the 1% to 10% level is required to deduce limits to a possible variation of each of these fundamental parameters by combining the results of several complementary clock comparisons.

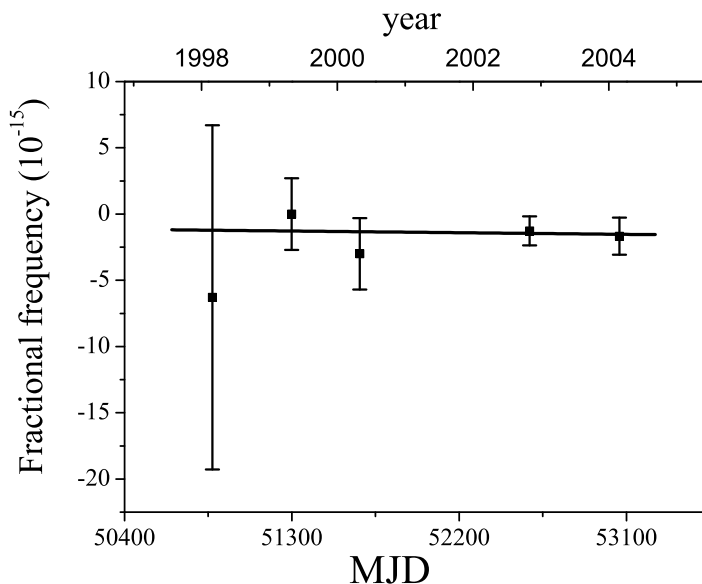


Figure 7: Measured ^{87}Rb frequencies referenced to the ^{133}Cs fountains over 72 months. The 1999 measurement value ($\nu_{\text{Rb}}(1999) = 6\,834\,682\,610.904\,333\text{ Hz}$) is conventionally used as reference. A weighted linear fit to the data (solid line) gives $\frac{d}{dt} \ln\left(\frac{\nu_{\text{Rb}}}{\nu_{\text{Cs}}}\right) = (-0.5 \pm 5.3) \times 10^{-16} \text{ yr}^{-1}$. MJD represent Modified Julian Dates.

Fig.7 summarizes the comparison between ^{87}Rb and ^{133}Cs hyperfine fundamental constants. The same applies to higher order terms in the expression of the hyperfine energy (1). A precision of 1 to 10 % on the sensitivity is sufficient to interpret current experiments.

quencies that have been performed using the above described fountain ensemble over a duration of 6 years. Each point on the graph summarizes the result of one to two months of measurements which include each time an evaluation of all known systematic effects [27, 43, 44]. A weighted linear fit to the data in Fig.7 determines how these measurements constrain a possible time variation of $\nu_{\text{Rb}}/\nu_{\text{Cs}}$. We find:

$$\frac{d}{dt} \ln \left(\frac{\nu_{\text{Rb}}}{\nu_{\text{Cs}}} \right) = (-0.5 \pm 5.3) \times 10^{-16} \text{ yr}^{-1} \quad (3)$$

which represents a 100-fold improvement over the $\text{Hg}^+\text{-H}$ hyperfine energy comparison [28]. This results implies the following constraint:

$$\frac{d}{dt} \ln \left(\frac{g_{\text{Cs}}}{g_{\text{Rb}}} \alpha^{0.49} \right) = (0.5 \pm 5.3) \times 10^{-16} \text{ yr}^{-1}. \quad (4)$$

Using the calculated link between g-factors and m_q , m_s and Λ_{QCD} (ref. [35, 36]), we find the following constraint to the variation of fundamental constants:

$$\frac{d}{dt} \ln \left(\alpha^{0.49} [m_q/\Lambda_{\text{QCD}}]^{0.174} [m_s/\Lambda_{\text{QCD}}]^{0.027} \right) = (0.5 \pm 5.3) \times 10^{-16} \text{ yr}^{-1}. \quad (5)$$

As pointed out in [25, 45, 46], the hypothetical unification of all interactions implies that a variation of the fine-structure constant α should be accompanied by a variation of the strong interaction constant and of elementary particle masses. Within this framework, current estimates gives [25, 36, 45, 46]:

$$\frac{\delta(m/\Lambda_{\text{QCD}})}{(m/\Lambda_{\text{QCD}})} \sim 35 \times \frac{\delta\alpha}{\alpha}. \quad (6)$$

Within this theoretical framework, the present comparison between Rb and Cs fountains (Eq. 3) constrains a time variation of α at the level of $7 \times 10^{-17} \text{ yr}^{-1}$. In the future, improvement of ^{87}Rb and ^{133}Cs fountain to accuracies of few parts in 10^{16} and repeated comparisons over several years between these devices will improve the above result by at least one order of magnitude.

The transportable fountain FOM has similarly been used as a primary standard in the measurement of the frequency ν_{H} of the hydrogen 1S-2S transition performed at Max-Planck Institut in Garching (Germany) [30, 47]. Two measurements performed over a 4 year period constrain fractional variations of $\nu_{\text{Cs}}/\nu_{\text{H}}$ at the level of $(3.2 \pm 6.3) \times 10^{-15} \text{ yr}^{-1}$. This constrains fractional variations of $g_{\text{Cs}}(m_e/m_p)\alpha^{2.83}$ at the same level [28, 37]. Combining these results with other recent comparisons ($^{199}\text{Hg}^+$ optical clock versus

^{133}Cs fountain [32, 48], $^{171}\text{Yb}^+$ optical clock versus ^{133}Cs fountain [33, 49]), it is possible to independently set limits on variations of α , $g_{\text{Rb}}/g_{\text{Cs}}$ and $g_{\text{Cs}}(m_e/m_p)$. These measurements test the stability of the electroweak interaction (α) and of the strong interaction ($g_{\text{Rb}}/g_{\text{Cs}}$, $g_{\text{Cs}}(m_e/m_p)$) separately [47, 49] and independently of any cosmological model.

5 The PHARAO cold atom space clock and ACES

PHARAO, as “Projet d’Horloge Atomique par Refroidissement d’Atomes en Orbite”, has started in 1993 with the objective of performing fundamental metrology with a space cold atom clock [50]. The combination of laser cooling techniques [51] and microgravity environment indeed allows the development of space clocks with unprecedented performances.

To demonstrate the feasibility of a compact cold atom clock operating in microgravity, BNM-SYRTE and LKB with the support of CNES (the French space agency) have undertaken the construction of a clock prototype in 1994. The prototype was successfully tested in 1997 in jet plane parabolic flights [9]. The same year, ESA, the European Space Agency, selected the ACES proposal (Atomic Clock Ensemble in Space) [52]. ACES will perform fundamental physics tests by using the PHARAO cold atom clock, a H-maser (developed by the Neuchâtel Observatory) and a time and frequency transfer system MWL on a platform developed by ESA. This ensemble will fly on board the international space station in 2008-2009. The station is orbiting at a mean elevation of 400 km with a 90 mn period and an inclination angle of 51.6° . The planned mission duration is 18 months. During the first 6 months, the performances of the PHARAO cold atom clock in space will be established. Thanks to the microgravity environment the linewidth of the atomic resonance will be varied by two orders of magnitude (from 11 Hz to 110 mHz). The target performance is $7 \times 10^{-14} \tau^{-1/2}$ for the frequency stability and 10^{-16} for the frequency accuracy. In the second part of the mission, the onboard clocks will be compared to a number of ground based clocks operating both in the microwave and the optical domain.

In 2001, PHARAO entered into industrial development under the management of CNES with the construction of two clock models, an engineering model for test and validation, and a flight model.

Figure 8: The PHARAO sub-systems and interfaces.

The PHARAO instrument

The clock is composed of four main sub-systems as shown in figure 8. Each sub-system has been subcontracted to different manufacturers and they will be assembled at CNES Toulouse to validate the clock operation.

The laser source provides all the laser tools for cooling, launching and detection of the atoms. Two extended cavity diode lasers [53] are used as master lasers. One of them injection-locks two slave diode lasers to provide high laser power for capturing $\sim 10^8$ in optical molasses. The second laser is used as a repumping laser. The two master laser frequencies are stabilized by servo-loops using absorption signals through cesium cells. The other laser frequencies are synthesized by using 6 acousto-optic modulators (AOM). These AOM also control the laser beam amplitudes. The output laser beams are connected to the cesium tube through polarization maintaining optical fibers. Figure 9 shows the PHARAO optical bench during the assembly. The total mass is 20 kg, the volume is 26 liters and the power consumption is 40 W.

The cesium tube provides the atomic source, the controlled environment for the atomic manipulation, the interrogation and detection process (figure 9). Its design is similar to atomic fountains except for the interrogation zone where a two zone Ramsey cavity is used. The Ramsey cavity (figure 11) has been specially developed for this application and forms a ring resonator. One coupling system feeds two symmetrical lateral waveguides which meet at the

Figure 9: The PHARAO optical bench during assembly. The bench surface is $55 \times 33 \text{ cm}^2$. The laser source includes 8 frequency stabilized diode lasers. The laser light for atom manipulation is coupled to the vacuum tube through optical fibers. (courtesy of EADS SODERN).

two interaction zones. The advantage of this configuration is to provide very weak phase disturbances of the internal microwave field while enabling large holes ($8 \times 9 \text{ mm}$) for the atom path. The flight model of the microwave cavity is currently mounted (September 2004) inside the atomic fountain FO1 to measure the end to end cavity phase shift before integration in the flight model. These measurements and numerical simulations, should enable us to determine the cavity phase shift effect with an accuracy of a few parts in 10^{17} .

The cesium tube is designed for a vacuum of 10^{-8} Pa in order to minimize the cold atom losses with the background gas collisions. Three layers of magnetic shields and a servo system maintain the magnetic field instability in the interaction zone below 20 pT . Similarly, the interaction zone temperature is regulated to better than 0.2°C .

The microwave chain synthesizes the two radiofrequency signals for the state selection cavity and the interrogation cavity. A 100 MHz VCXO (Voltage Control Oscillator) is phase-locked to an Ultra Stable Oscillator (USO) for the short term stability and to the Space Hydrogen Maser (SHM) for the medium term. Three USOs have been space qualified for our application. We have compared these quartz oscillators to the BNM-SYRTE CSO. Their

Figure 10: Cross-section of the cesium tube. The mass is 45 kg and the volume 70 liters.

frequency stability is on the order of 7×10^{-14} from 1 to 10 s integration time. The engineering model of the chain has been fully tested and the results are in agreement with the performance objectives of the space clock. A further performance verification is currently being made by using the microwave source in the FO2 fountain. All PHARAO sub-systems are driven and controlled by a computer (UGB, On Board Data Processing Unit). The UGB also manages the data flux between the clock and the ACES payload. When assembled, the clock fills a volume of about 200 l for a weight of 91 kg and an electric consumption of 114 W.

The final assembly of the engineering model of the PHARAO clock will start at the end of 2005 at CNES-Toulouse. After the clock functional and performance test are made, the flight model will be assembled and finally tested. For both models, we expect to reach 10^{-15} frequency accuracy in the Earth gravity environment and 10^{-16} in microgravity environment.

Scientific objectives of the ACES mission

The objectives of PHARAO/ACES are (i) to explore and demonstrate the high performances of the cold atom space clock (ii) to achieve time and frequency transfer with stability better than 10^{-16} and (iii) to perform fundamental physics tests. A detailed account can be found in [54].

The combination of PHARAO with SHM will define an on board fre-

Figure 11: The Ramsey interrogation cavity. The cavity in pure copper is screwed on a rigid structure to avoid deformation during launch. The length of the cavity is 280 mm. The atoms enter the cavity through the cut-off waveguide with a rectangular shape (on the left). Also visible in the center is the the microwave coupling system. (Courtesy of EADS SODERN and TAS).

quency reference having a long term stability and accuracy provided by PHARAO and a short term stability determined by SHM. The resulting fluctuations of ACES frequency reference are expected to be about 10 ps per day. The orbit of ISS will allow ground users to compare and synchronize their own clock to ACES clocks, leading to a worldwide access to the ultra stable frequency reference of ACES. The results of these comparisons at 10^{-16} level will provide new tests in fundamental physics such as an improved measurement of Einstein's gravitational red-shift, a search for a possible anisotropy of the speed of light and a search for possible space-time variations of fundamental physical constants, similar to that described above in section 4. The current most precise measurement of the red-shift was made by the space mission Gravitational Probe A (GPA) with an accuracy of 7×10^{-5} [55]. PHARAO/ACES will improve this test by a factor 30. By allowing worldwide comparison between distant clocks, operating with different atomic species, ACES will play a major role in establishing new limits for variations of fundamental constants.

Finally, PHARAO/ACES will be a pioneering cold atom experiment in

space. The PHARAO technology can be extended for the development of a new generation of high performance inertial sensors and clocks using matter wave interferometry. As for atomic clocks, such sensors may achieve extremely high sensitivity in micro-gravity environment, as pointed out in the ESA HYPER project [56]. These instruments could then be used for a large variety of scientific space missions such as VLBI, gravitational wave detection, and deep space navigation.

6 Conclusions

With methods described in this paper, we expect to bring the accuracy of ^{133}Cs fountains at 1 or 2 parts in 10^{16} . For ^{87}Rb , a frequency stability of $1 \times 10^{-14} \tau^{-1/2}$ i.e. 3×10^{-17} at one day seems accessible, together with an excellent accuracy. Routine operation of these devices over several years will have a profound impact on ultra-precise time keeping and fundamental physics tests. To take full benefit of this performance, long distance time transfer systems must be upgraded. In particular, the ACES time and frequency transfer system will enable comparisons at the level of 10^{-16} per day in 2008-2009. Another route currently under study makes use of telecom optical fibers and over 100 km distance a stability of 1×10^{-14} at 1 s and 2×10^{-17} at one 1 day has already been demonstrated [57]. Extension to larger distances is under study.

More generally, clocks operating in the optical domain rather than in the microwave domain are making rapid progress on the ground [58]. The frequency of these clocks is four to five orders of magnitude higher than the frequency of microwave standards and with an equivalent linewidth, the quality factor of the resonance exceeds that of cesium clocks by the same factor. Using laser cooled atoms or ions and ultra-stable laser sources [59], these optical clocks will likely open the $10^{-17} - 10^{-18}$ stability range. Using the wide frequency comb generated by femtosecond lasers, it is now possible to connect virtually all frequency standards together throughout the microwave to ultra-violet frequency domain [48, 60]. The attractive proposal of [61, 62] to realize an optical lattice clock is currently receiving a great deal of interest. In this method, neutral atoms are confined in an optical lattice in the Lamb-Dicke regime. Light-shifts of the clock levels induced by the lattice beams are differentially compensated at an appropriate laser detuning. This proposal combines several interesting features such as long observation time, large number of atoms, and recoil-free resonance [63]. Promising atoms to implement this method are alkaline-earth atoms because of their strongly forbidden inter-combination line. Ca [48, 64], Sr [63, 65] and Yb [66, 67, 68]

are actively studied.

In the frequency stability range of $10^{-17} - 10^{-18}$, it is clear that fluctuations of the Earth potential at the clock location induced, for instance, by sea tides will affect comparisons between distant clocks. This limitation could be turned into an advantage if one installs such ultra-stable clock in space where the gravitational potential can present far reduced fluctuations compared to ground. As in the past, clocks with very high stability will have an ever increasing impact on scientific and industrial applications.

7 Acknowledgements

BNM-SYRTE and Laboratoire Kastler Brossel are Unités Associées au CNRS, UMR 8630 and 8552. This work was supported in part by BNM, CNRS, CNES and ESA. P. Wolf is on leave from Bureau International des Poids et Mesures, Pavillon de Breteuil, 92312 Sèvres Cedex, France. J. Grünert and L. Cacciapuoti acknowledge financial support from the CAUAC European Research Training Network.

References

- [1] See, for instance, the 1997 Nobel lectures by Steven Chu, C. Cohen-Tannoudji and W. Phillips in *Reviews of Modern Physics* 70, 685 (1998)
- [2] See for instance, C. Will, *Theory and experiment in gravitational physics*, Cambridge University Press, (1993).
- [3] See for instance *Proceedings of the 6th Symposium on Frequency Standards and Metrology*, Gill P. ed., World Scientific, Singapore, 2001.
- [4] H. Margolis, G. Barwood, G. Huang, H. Klein, S. Lea, K. Szymaniec, P. Gill, *Science* **306**, 1355 (2004)
- [5] Clairon A. et al., A cesium fountain frequency standard: recent results, *IEEE Trans. Instrum. Meas.* 44 (1995) 128.
- [6] Bordé C.J., *Atomic Clocks and Inertial Sensors*, *Metrologia* 39 (2002) 435.
- [7] Sortais Y. et al., Cold Collision Frequency Shifts in a ^{87}Rb Fountain, *Phys. Rev. Lett.* 85 (2000) 3117.

- [8] Fertig C., Gibble K., Measurement and Cancellation of the Cold Collision Frequency Shift in an ^{87}Rb Fountain Clock, *Phys. Rev. Lett.* 85 (2000) 1622.
- [9] Laurent P. et al., A cold atom clock in absence of gravity, *Eur. Phys. J. D* 3 (1998) 201.
- [10] Mann A.G., Chang S. and Luiten A.N., Cryogenic Sapphire Oscillator with Exceptionally High Frequency Stability, *IEEE Trans. Instrum. Meas.* 50 (2001) 519.
- [11] Vian C. et al., BNM-SYRTE Fountains: Recent Results, submitted to *IEEE Trans. Instrum. Meas.* (2004).
- [12] Gibble K., Chu S., A laser cooled Cs Frequency Standard and a Measurement of the Frequency Shift due to Ultra-cold Collisions, *Phys. Rev. Lett.* 70 (1993) 1771.
- [13] Ghezali S., Laurent P., Lea S.N., Clairon A., An Experimental Study of the Spin-Exchange Frequency Shift in a Laser Cooled Cesium Fountain Standard, *Europhys. Lett.* 36 (1996) 25.
- [14] Pereira Dos Santos F. et al., Controlling the Cold Collision Shift in High Precision Atomic Interferometry, *Phys. Rev. Lett.* 89 (2002) 233004.
- [15] Bize S. et al., Cavity Frequency Pulling in Cold Atom Fountains, *IEEE Trans. Instrum. Meas.* 50 (2001) 503.
- [16] Marion H. et al., First Observation of Feshbach Resonances at Very Low Magnetic Field in a ^{133}Cs Fountain, *Proc. of the 2004 EFTF* (2004) arxiv:physics/0407064.
- [17] Schröder R., Hübner U., Griebisch D., Design and realization of the microwave cavity in the PTB caesium atomic fountain clock CSF1, *IEEE Trans. Ultrason. Ferroelect. Freq. Contr.* 49 (2002) 383.
- [18] Parker T.E. et al., First Comparison of Remote Cesium Fountains, *Proc. of the 2001 IEEE Intl. Freq. Cont. Symp.* (2001) 63.
- [19] Richard J.-Y. et al., Comparison of remote cesium fountains using GPS P3 and TWSTFT links, *Proc. of the 2004 EFTF* (2004).
- [20] Damour T., Dyson F., The Oklo bound on the time variation of the fine-structure constant revisited, *Nucl. Phys. B* 480 (1996) 37.

- [21] Fujii Y., Time-variability of the fine-structure constant expected from the Oklo constraint and the QSO absorption lines, *Phys. Lett. B* 573 (2003) 39.
- [22] Webb J.K. et al., Further Evidence for Cosmological Evolution of the Fine Structure Constant, *Phys. Rev. Lett.* 87 (2001) 091301.
- [23] Srianand R., Chand H., Petitjean P., Aracil B., Limits on the Time Variation of the Electromagnetic Fine-Structure Constant in the Low Energy Limit from Absorption Lines in the Spectra of Distant Quasars, *Phys. Rev. Lett.* 92 (2004) 121302.
- [24] Marciano W.J., Time Variation of the Fundamental “Constants” and Kaluza-Klein Theories, *Phys. Rev. Lett.* 52 (1984) 489.
- [25] Damour T., Polyakov A., The String Dilaton and a Least Coupling Principle, *Nucl. Phys. B* 423 (1994) 532.
- [26] Damour T., Piazza F., Veneziano G., Runaway Dilaton and Equivalence Principle Violations, *Phys. Rev. Lett.* 89 (2002) 081601.
- [27] Marion H. et al., Search for Variations of Fundamental Constants using Atomic Fountain Clocks, *Phys. Rev. Lett.* 90 (2003) 150801.
- [28] Prestage J.D., Tjoelker R.L., Maleki L., Atomic Clocks and Variations of the Fine Structure Constant, *Phys. Rev. Lett.* 74 (1995) 3511.
- [29] Berkeland D.J. et al., Laser-Cooled Mercury Ion Frequency Standard, *Phys. Rev. Lett.* 80 (1998) 2089.
- [30] Niering M. et al., Measurement of the Hydrogen 1S-2S Transition Frequency by Phase Coherent Comparison with a Microwave Cesium Fountain Clock, *Phys. Rev. Lett.* 84 (2000) 5496.
- [31] Helmcke J. et al., Optical Frequency Standard Based on Cold Ca Atoms, *IEEE Trans. Instrum. Meas.* 52 (2003) 250.
- [32] Bize S. et al., Testing the Stability of Fundamental Constants with the $^{199}\text{Hg}^+$ Single-Ion Optical Clock, *Phys. Rev. Lett.* 90 (2003) 150802.
- [33] Stenger J. et al., Absolute Frequency Measurement of the 435.5 nm $^{171}\text{Yb}^+$ Clock Transition with a Kerr-lens Mode-locked Femtosecond Laser, *Opt. Lett.* 26 (2001) 1589.

- [34] Peik E. et al., in Proc. of the Joint Mtg. IEEE Intl. Freq. Cont. Symp. and EFTF Conf. (2003).
- [35] Flambaum V.V., (2003) arxiv:physics/0302015.
- [36] Flambaum V.V., Leinweber D.B., Thomas A.W., Young R.D., Limits on the Temporal Variation of the Fine Structure Constant, Quark Masses and Strong Interaction from Quasar Absorption Spectra and Atomic Clock Experiments, Phys. Rev. D 69 (2004) 115006.
- [37] Dzuba V.A. , Flambaum V.V.,Webb J.K., Calculations of the Relativistic Effects in Many-electron Atoms and Space-time Variation of Fundamental Constants, Phys. Rev. A 59 (1999) 230.
- [38] Dzuba V.A. , Flambaum V.V., Webb J.K., Space-Time Variation of Physical Constants and Relativistic Corrections in Atoms, Phys. Rev. Lett. 82 (1999) 888.
- [39] Dzuba V.A., Flambaum V.V., Webb J.K., Atomic Optical Clocks and Search for Variation of the Fine-Structure Constant, Phys. Rev. A 61 (2000) 034502.
- [40] Karshenboim S.G. , Some Possibilities for Laboratory Searches for Variations of Fundamental Constants, Can. J. Phys. 78 (2000) 639.
- [41] Dzuba V.A., Flambaum V.V., Marchenko M.V., Relativistic Effects in Sr, Dy, YbII and YbIII and Search for Variation of the Fine Structure Constant, Phys. Rev. A 68 (2003) 022506.
- [42] Angstromann E.J., Dzuba V.A., Flambaum V.V., Relativistic Effects in Two Valence-electron Atoms and Ions and the Search for Variation of the Fine-structure Constant, Phys. Rev. A 70 (2004) 014102.
- [43] Bize S. et al., High-accuracy Measurement of the ^{87}Rb Ground-state Hyperfine Splitting in an Atomic Fountain, Europhys. Lett. 45 (1999) 558.
- [44] Bize S. et al., in Proc. of the 6th Symposium on Frequency Standards and Metrology, Gill P. ed., World Scientific, Singapore (2001) 53.
- [45] Calmet X., Fritzsche H., The Cosmological Evolution of the Nucleon Mass and the Electroweak Coupling Constants, Eur. Phys. J. C 24 (2002) 639.

- [46] Langacker P., Segre G., Strassler M.J., Implications of Gauge Unification for Time Variation of the Fine Structure Constant, *Phys. Lett. B* 528 (2002) 121.
- [47] Fischer M. et al., New Limits on the Drift of Fundamental Constants from Laboratory Measurements, *Phys. Rev. Lett.* 92 (2004) 230802.
- [48] Udem Th. et al., Absolute Frequency Measurements of Hg⁺ and Ca Optical Clock Transitions with a Femtosecond Laser, *Phys. Rev. Lett.* 86 (2001) 4996.
- [49] Peik E. et al., New Limit on the Present Temporal Variation of the Fine Structure Constant, (2004) arxiv:physics/0402132.
- [50] Laurent P. et al., Cesium fountains and micro-gravity clocks, in *Proc. of the 25th Moriond Conf. on Dark Matter in Cosmology, Clocks and Tests of Fundamental Laws* (1995).
- [51] See for instance *J. Opt. Soc. Am. B* (special issue) 6 (1989) 2020.
- [52] Salomon C., Veillet C., ACES: Atomic Clock Ensemble in Space, *Proc. of the 1st ESA symposium on Space Station Utilization, SP385* (1996) 295 .
- [53] Allard F., Maksimovic I., Abgrall M., Laurent P., Automatic system to control the operation of an extended cavity diode laser, *Rev. Sci. Instrum.* 75 (2004) 54.
- [54] Salomon C. et al., Cold Atoms in space and atomic clocks : ACES, *C.R. Acad. Sci. Paris, T2 Série 4* (2001) 1313.
- [55] Vessot R.F.C. et al., Tests of Relativistic Gravitation with a Spaceborne Hydrogen Maser, *Phys. Rev. Lett.* 45 (1980) 2081.
- [56] HYPER: Hyper-Precision Cold Atom Interferometry in Space, *ESA-SCI* (2000) 10.
- [57] Narbonne F. et al., *Proc. of the 2004 EFTF conf.* (2004).
- [58] See for instance *Proc. of the 2003 IFCS-EFTF conf.* (2003).
- [59] Young B.C., Cruz F.C., Itano W.M., Bergquist J.C., Visible Lasers with Subhertz Linewidths, *Phys. Rev. Lett.* 82 (1999) 3799.
- [60] Udem Th., Holzwarth R., Hänsch T.W., Optical frequency metrology, *Nature* 416 (2002) 233.

- [61] Katori H., Spectroscopy of strontium atoms in the Lamb-Dicke confinement, Proc. of the 6th Symposium on Frequency Standards and Metrology, Gill P. ed., World scientific, Singapore (2001) 323.
- [62] H. Katori, M. Takamoto, V.G. Pal'chikov, V.D. Ovsiannikov, Ultra-stable optical clock with neutral atoms in an Engineered light shift Trap, Phys. Rev. Lett. 91 (2003) 173005.
- [63] Takamoto M., Katori H., Spectroscopy of the 1S_0 - 3P_0 clock transition of ^{87}Sr in an optical lattice, Phys. Rev. Lett. 91 (2003) 223001.
- [64] Stenger J. et al., Phase-coherent frequency measurement of the Ca intercombination line at 657 nm with a Kerr-lens mode-locked femtosecond laser, Phys. Rev. A 63 (2001) 021802.
- [65] Courtilot I. et al., Clock transition for a future optical frequency standard with trapped atoms, Phys. Rev. A 68 (2003) 030501.
- [66] Kuwamoto T., Honda K., Takahashi Y., Yabuzaki T., Magneto-optical trapping of Yb atoms using an intercombination transition, Phys. Rev. A 60 (1999) R745.
- [67] Park C.Y., Yoon T. H., Efficient magneto-optical trapping of Yb atoms with a violet laser diode, Phys. Rev. A 68 (2003) 055401.
- [68] Porsev S.G., Derevianko A., Fortson E.N., Possibility of an optical clock using the $6\ ^1S_0$ - $6\ ^3P_0$ transition in $^{171,173}\text{Yb}$ atoms held in an optical lattice, Phys. Rev. A 69 (2004) 021403.

